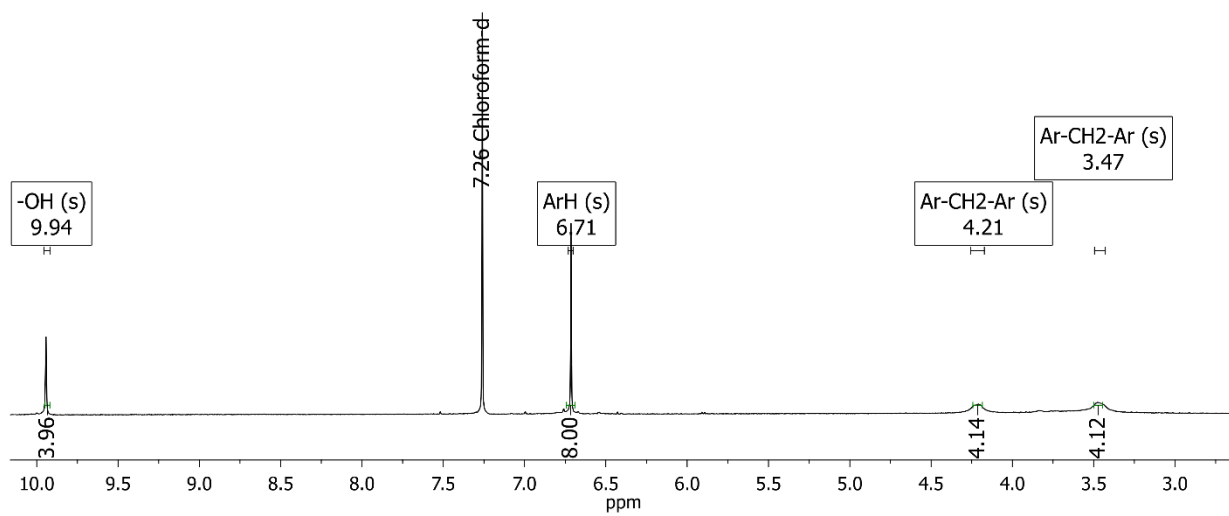
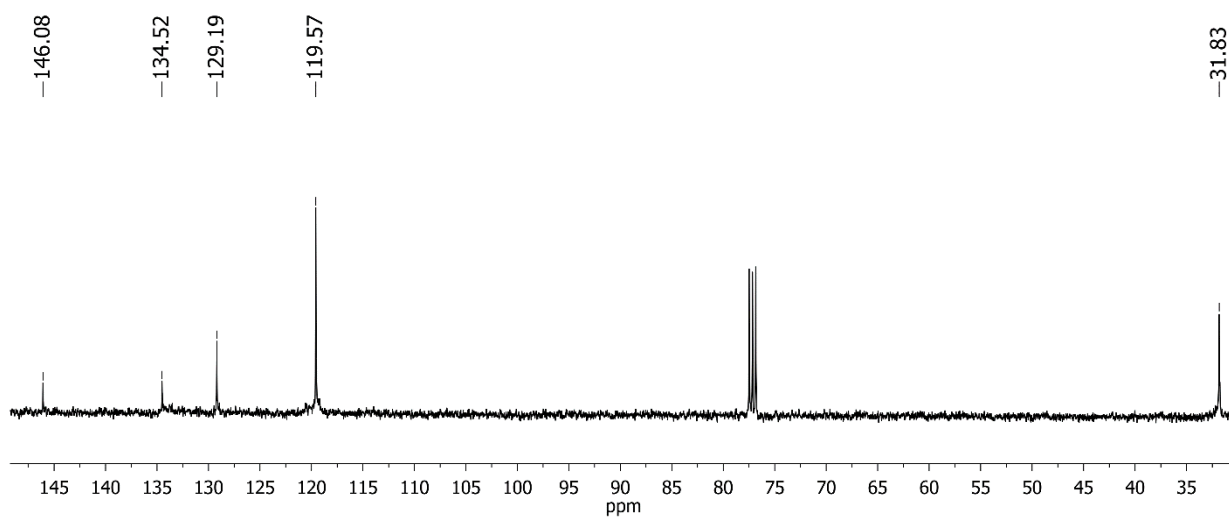


Supplementary Material

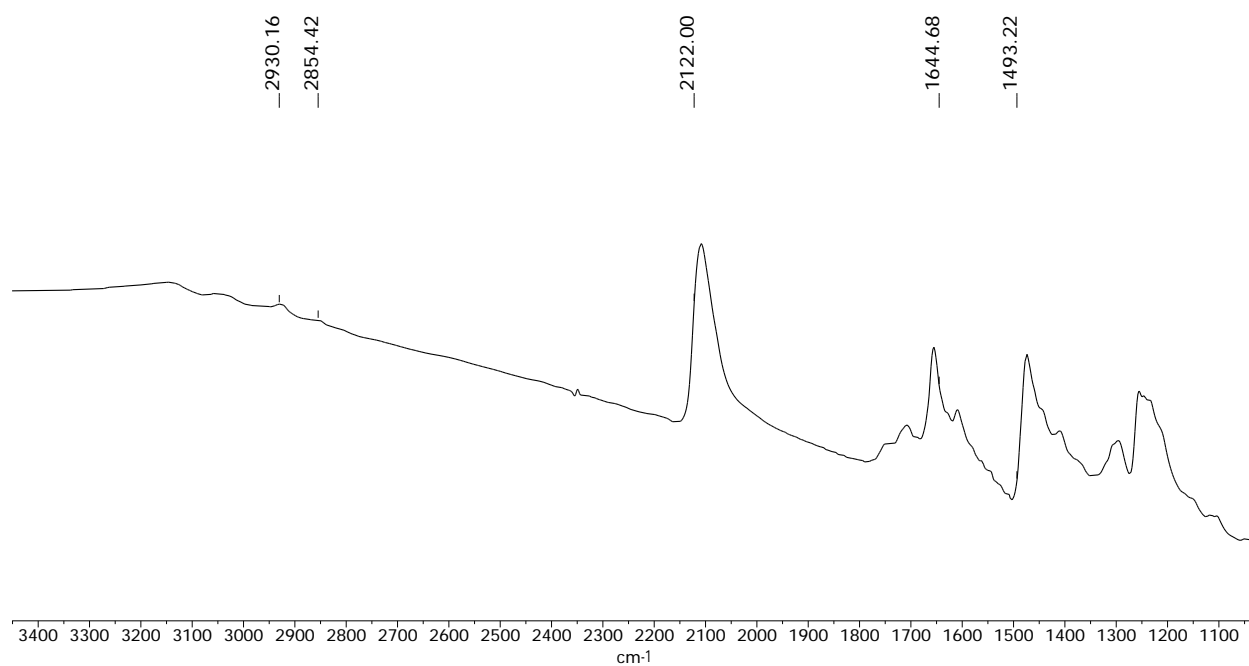
(a)



(b)



(c)



(d)

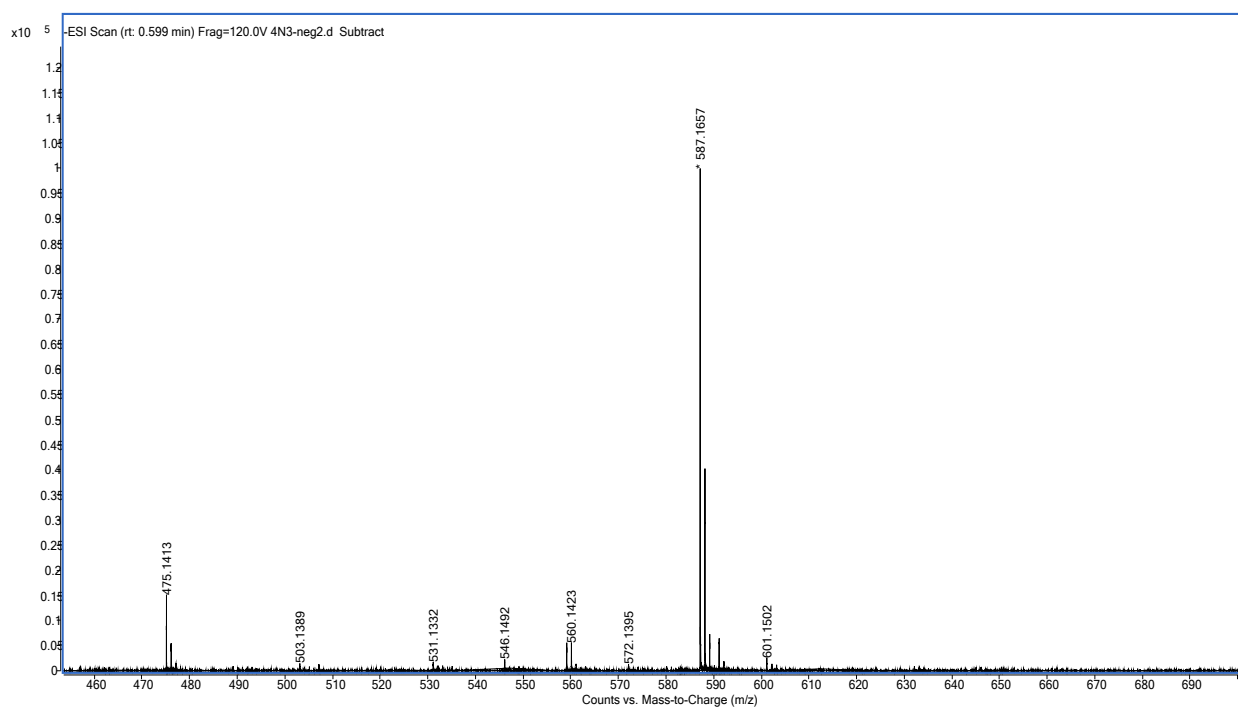
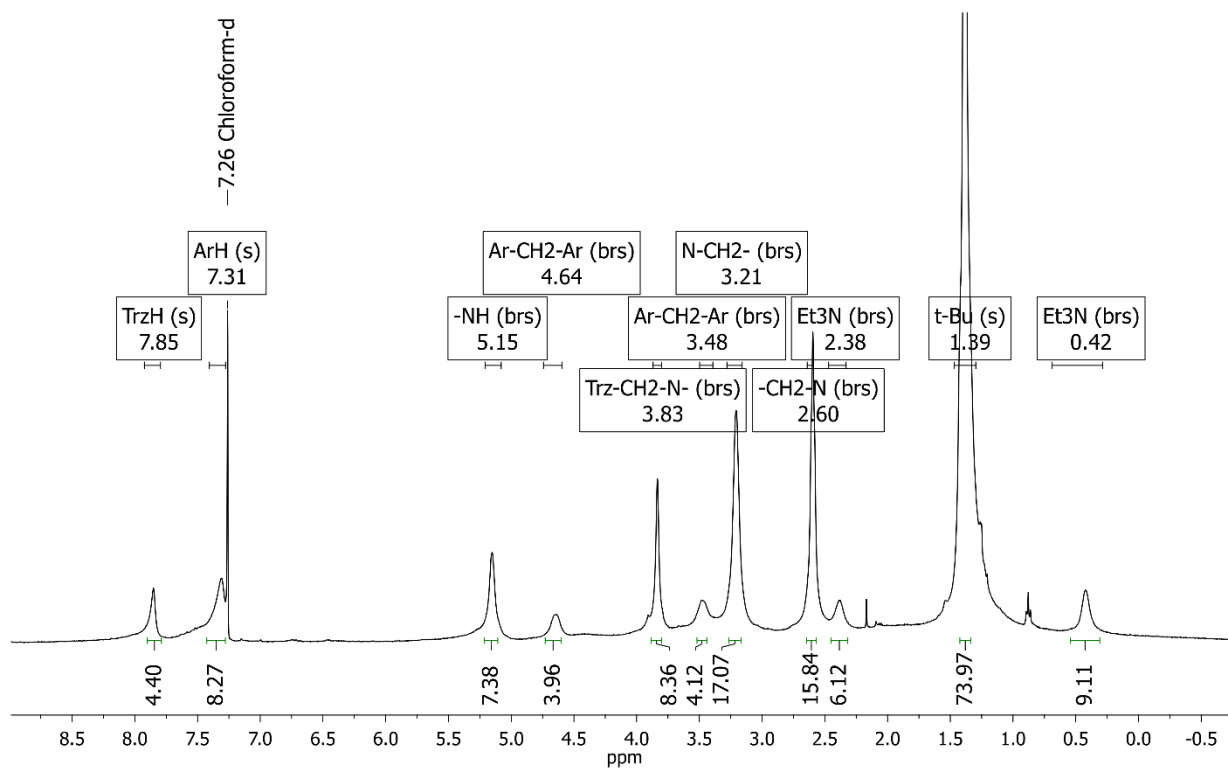
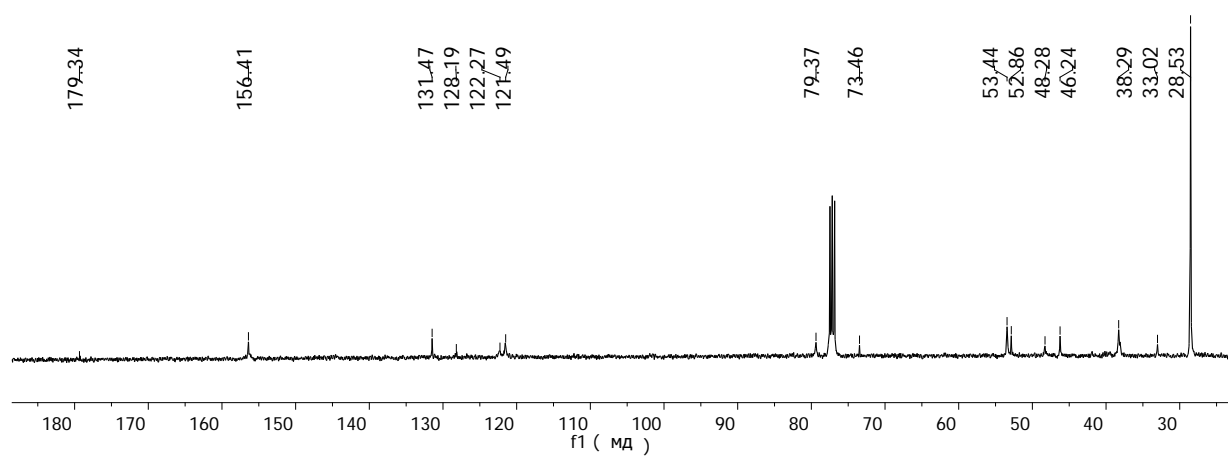


Figure S1. NMR ¹H (a), ¹³C (b), FTIR (c) and HRESI MS (d) spectra of 5,11,17,23-tetraazide-25,26,27,28-tetrahydroxycalix[4]arene **3**.

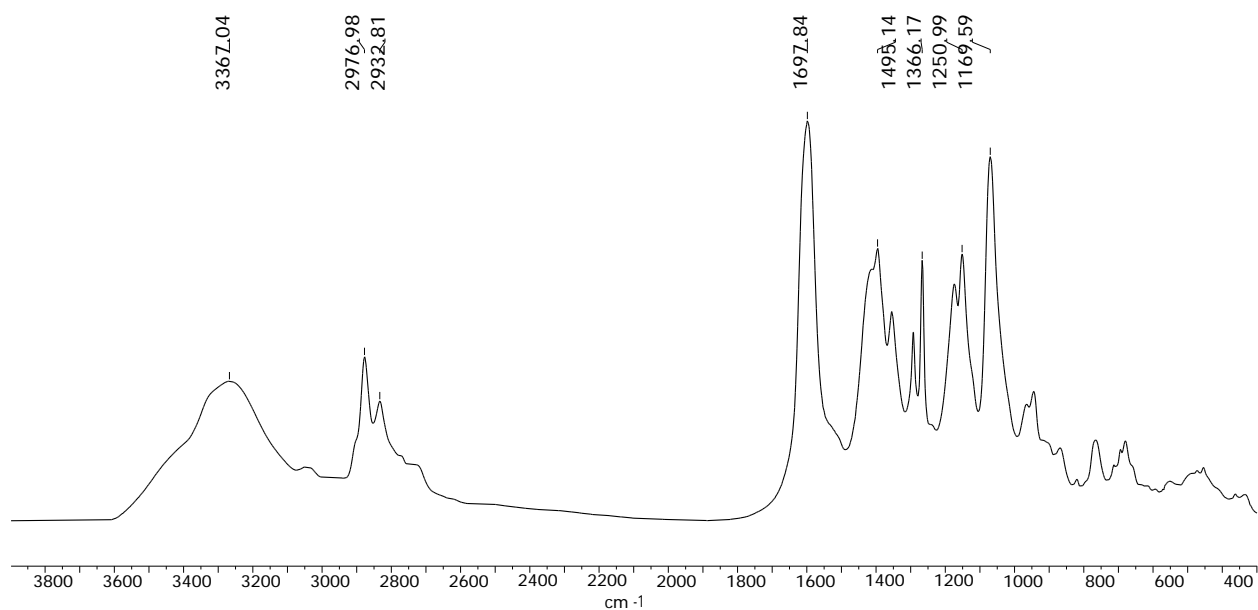
(a)



(b)



(c)



(d)

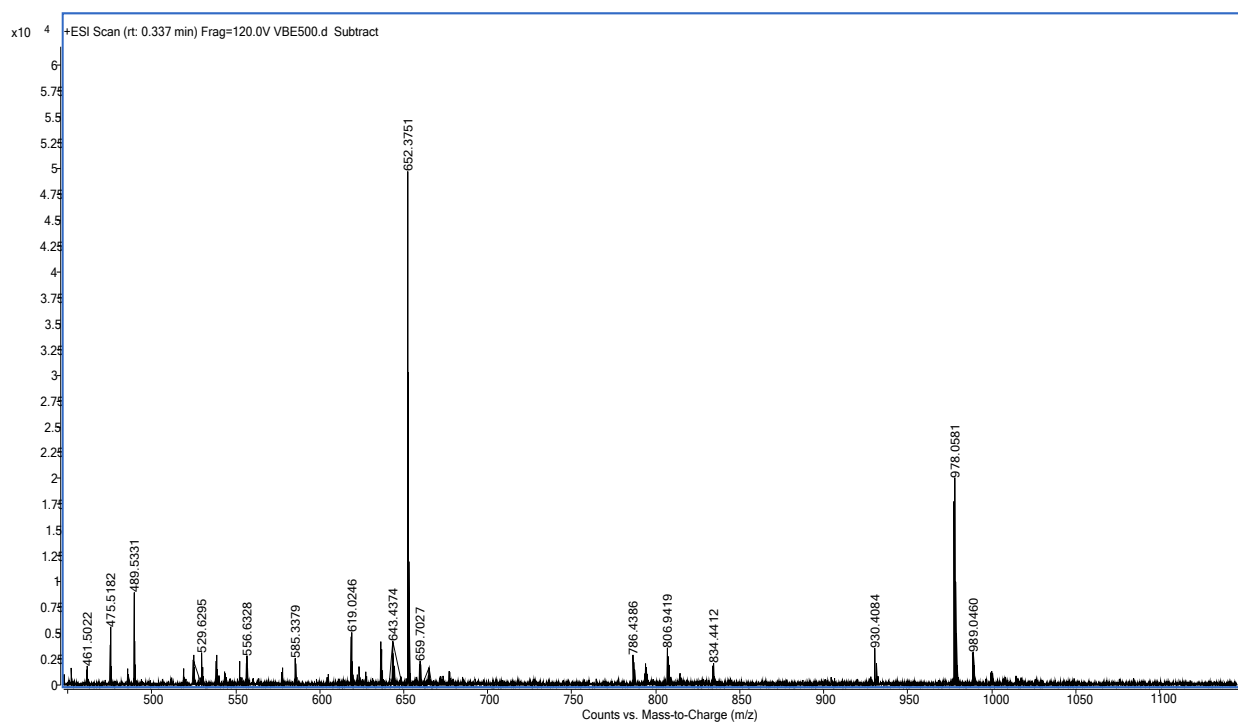
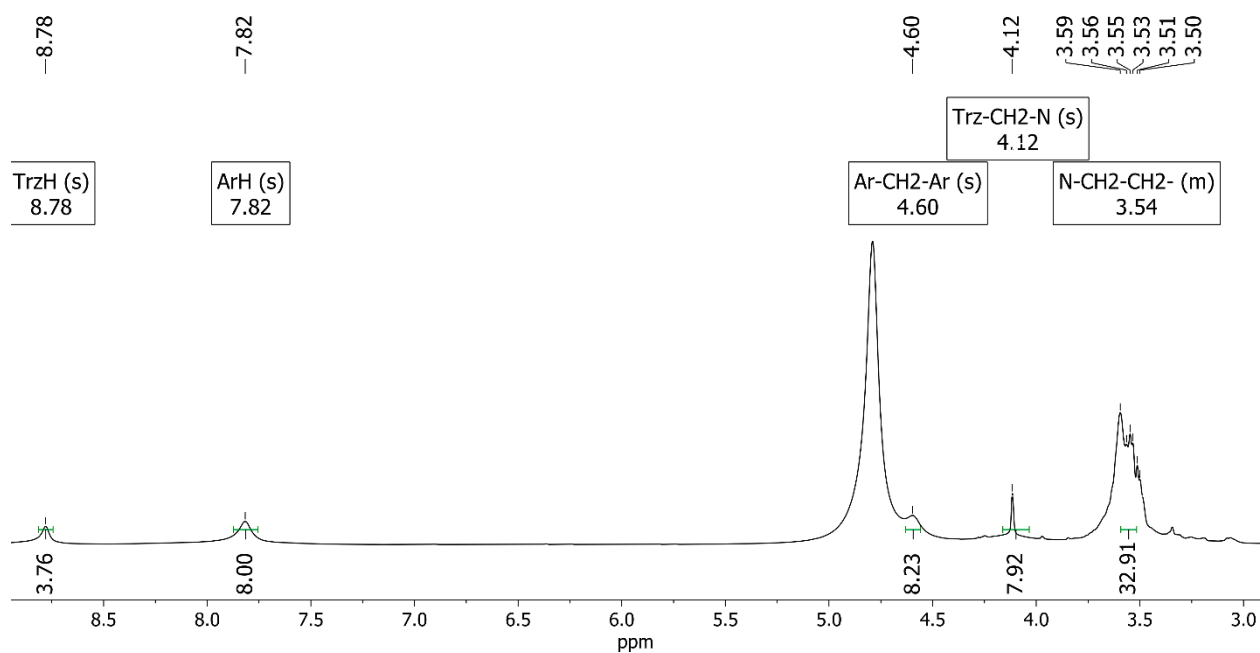
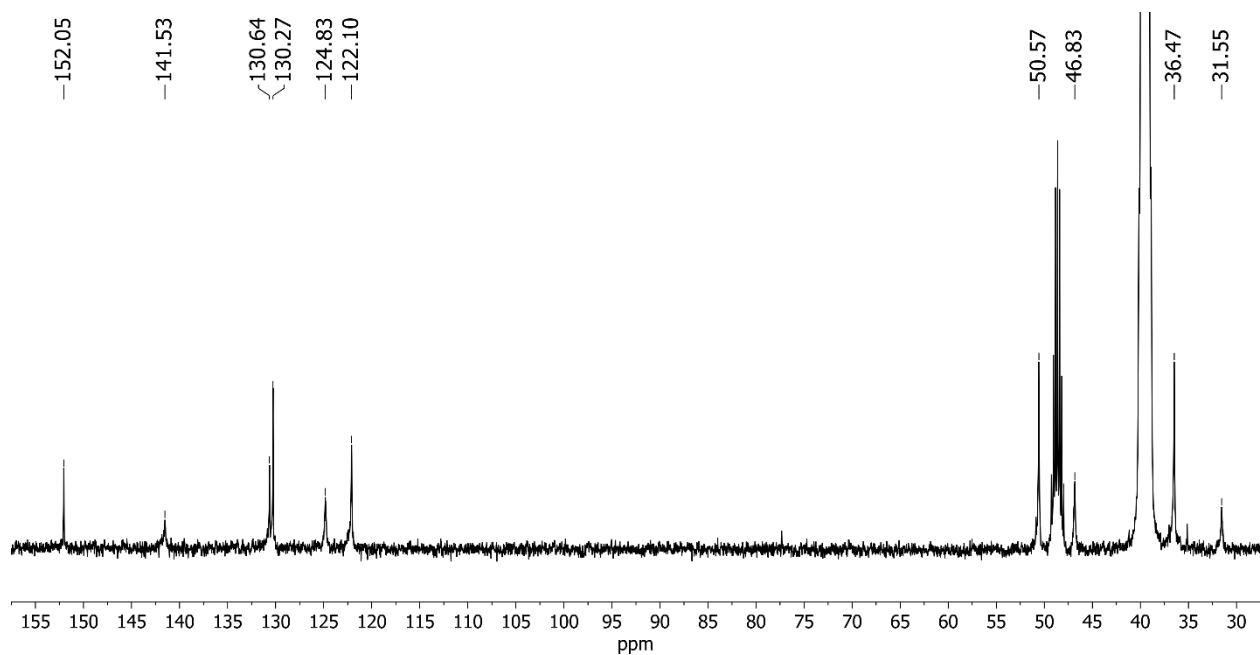


Figure S2. NMR ¹H (a), ¹³C (b), FT IR (c) and HRESI MS (d) spectra of (5,11,17,23-tetra(4-((bis(2-((tert-butoxycarbonyl)amino)ethyl)amino)methyl)-1H1,2,3-triazol-1-yl))-25,26,27,28-tetrahydroxycalix[4]arene) **4**.

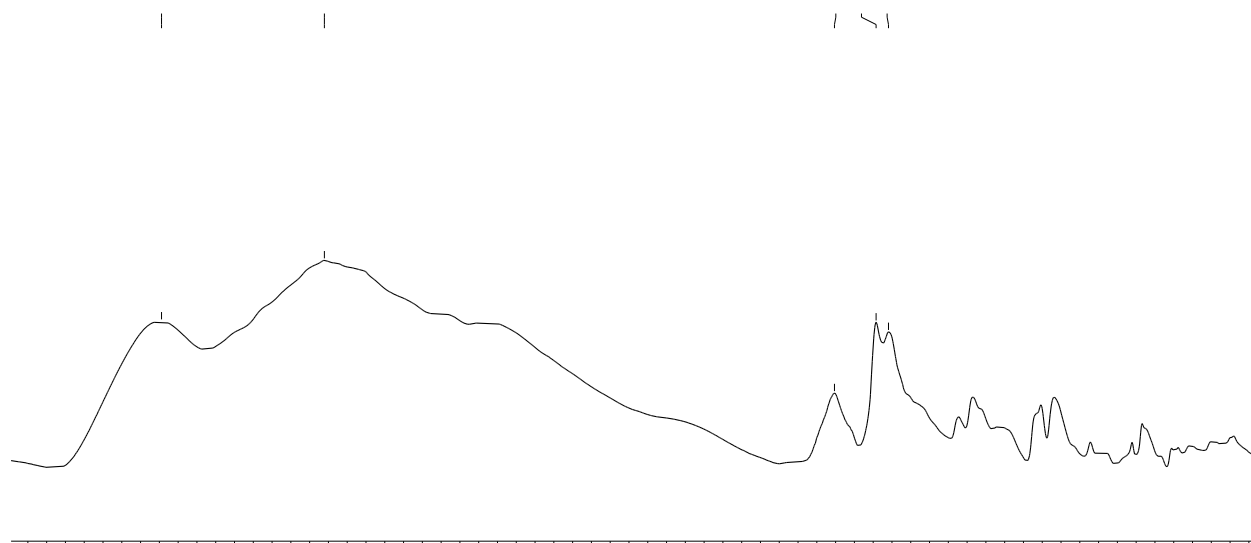
a)



b)



(c)



(d)

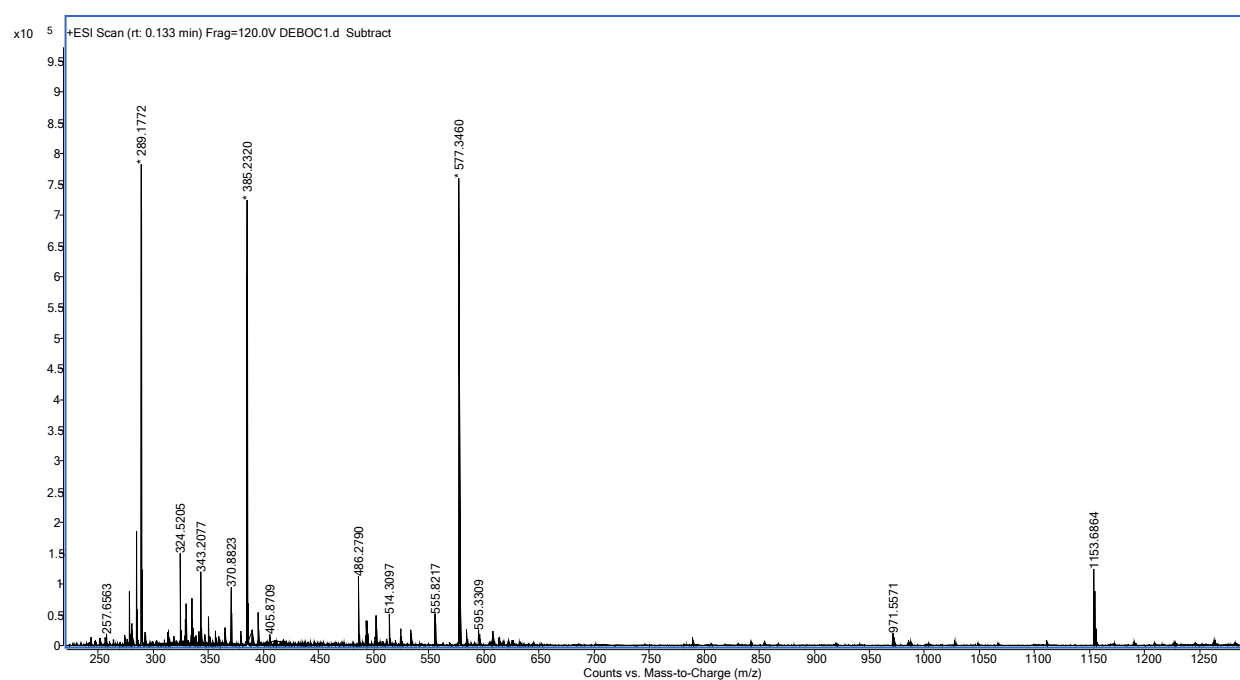
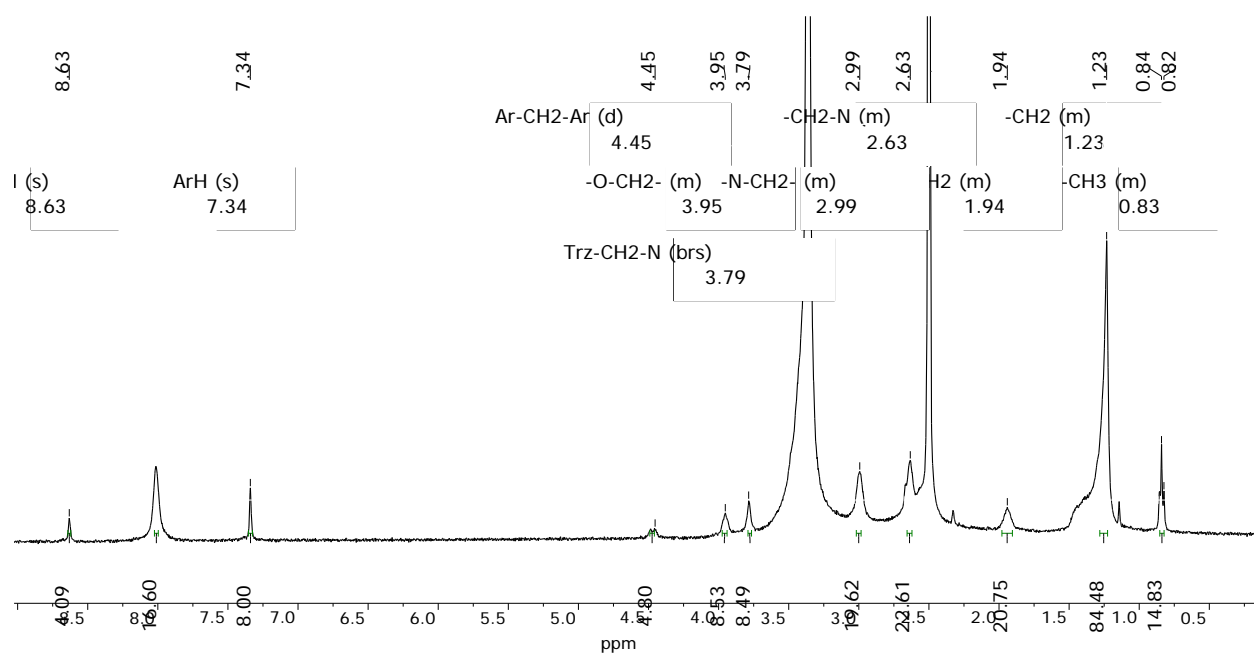
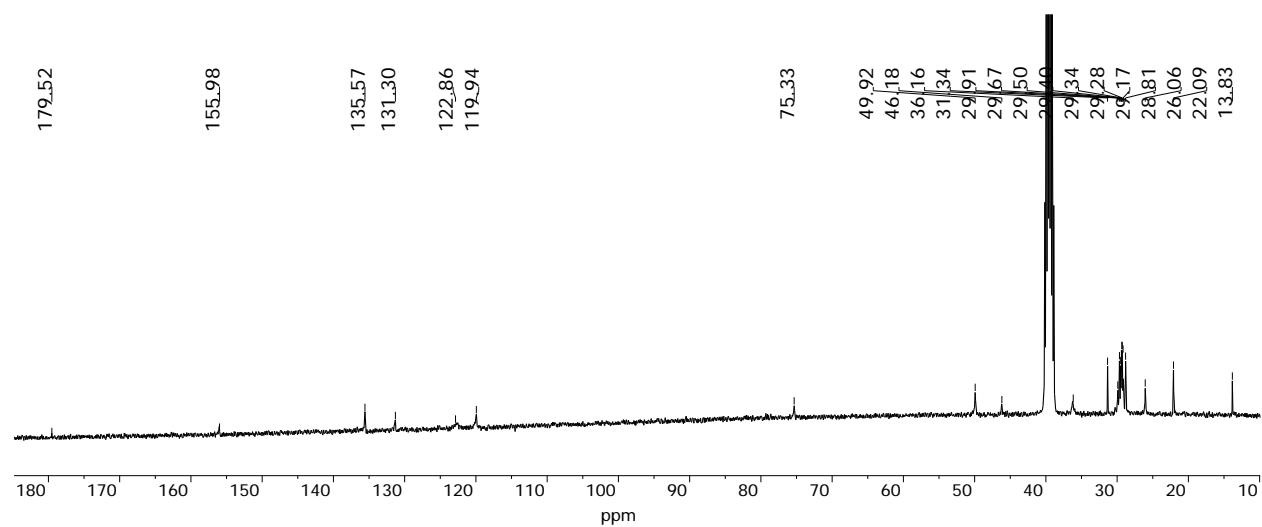


Figure S3. NMR ^1H (a), ^{13}C (b), FTIR (c) and ESI (d) spectra of (5,11,17,23-tetra(4-((bis(2-(amino)ethyl) amino)methyl)-1H-1,2,3-triazol-1-yl))- 25,26,27,28-tetrahydroxycalix[4]arene octahydrochloride)**5**.

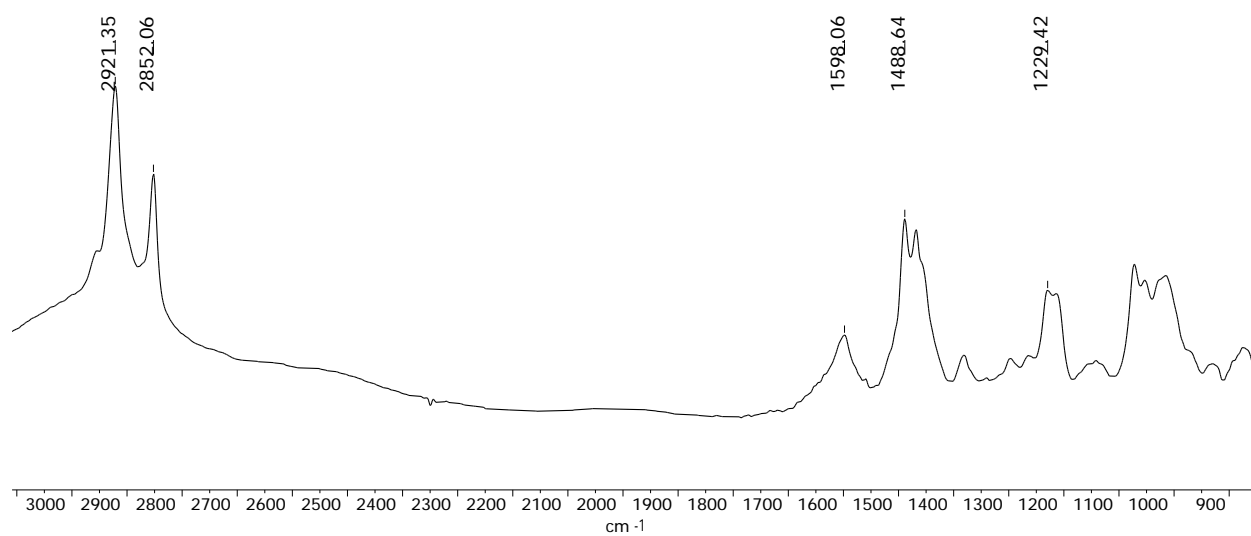
(a)



(b)



(c)



(d)

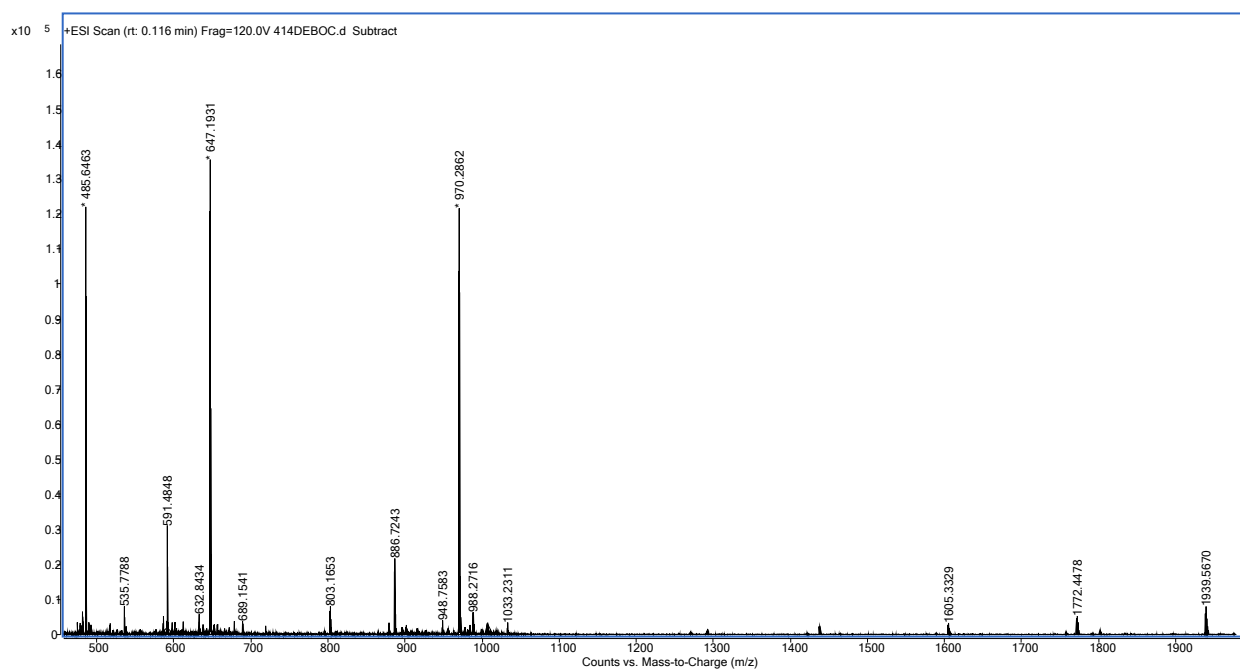


Figure S4. NMR ¹H (a), ¹³C (b), FTIR (c) and ESI (d) spectra of (5,11,17,23-tetra(4-((bis(2-(amino)ethyl) amino)methyl)-1H-1,2,3-triazol-1-yl))- 25,26,27,28-tetratetradecylcalix[4]arene octahydrochloride) **7**.

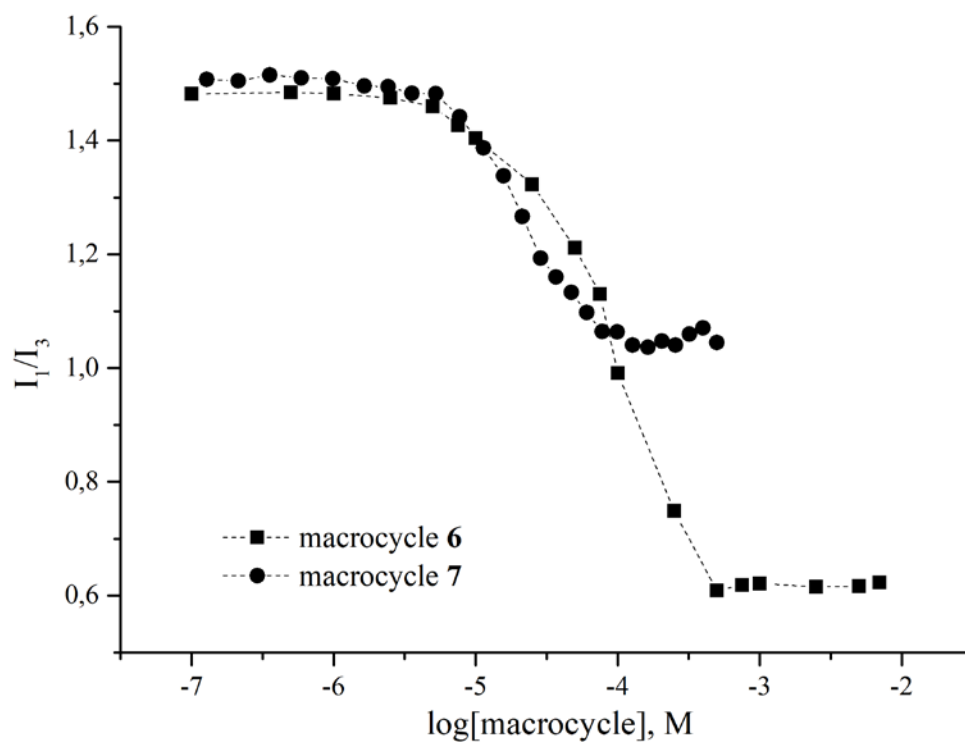


Figure S5. Dependence of the ratio of the first and third pyrene emission peaks on the logarithm of the concentration of macrocycles **6**, **7**.

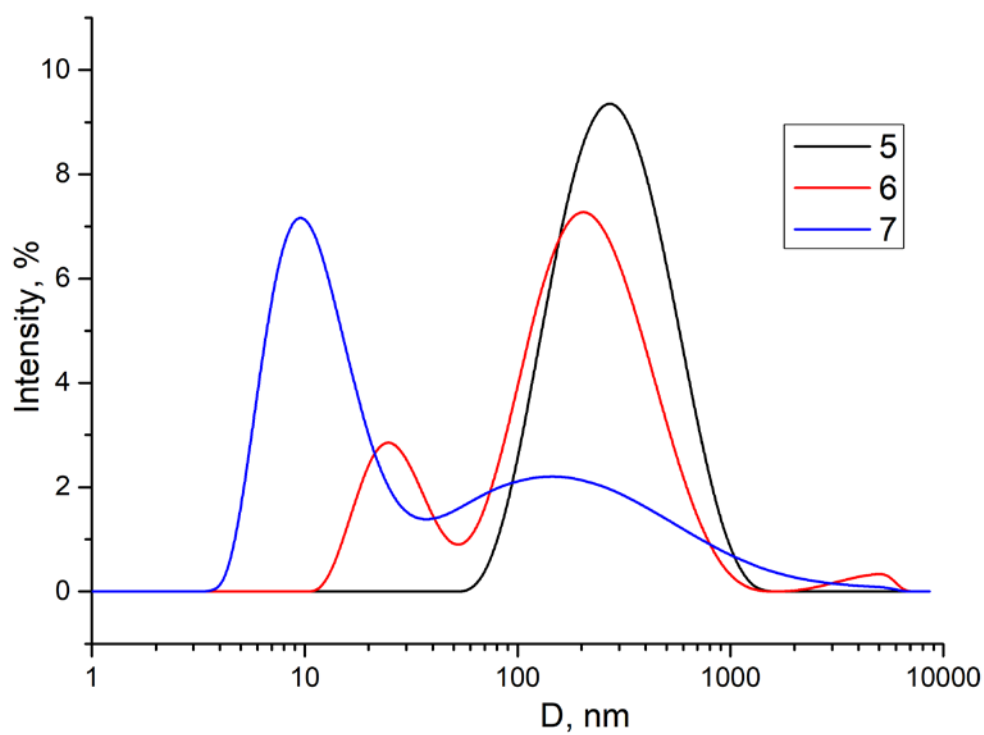
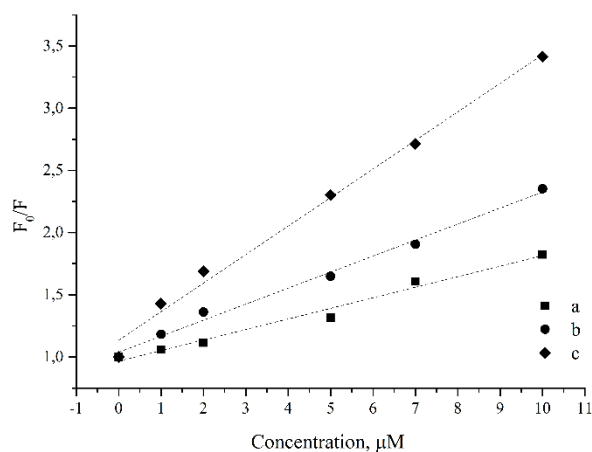
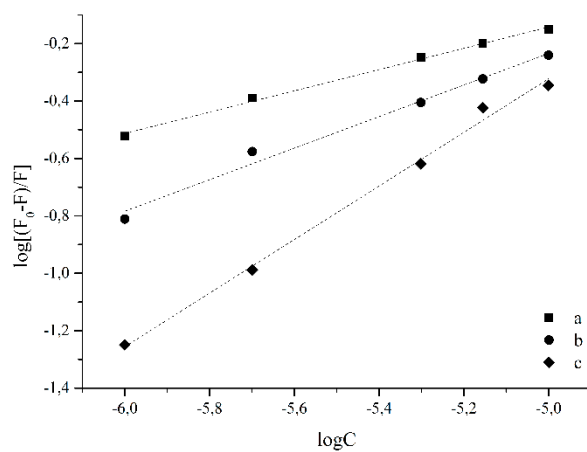


Figure S6. DLS intensity vs D graph for solutions of **5-7** ($C = 0.05$ mM, 10 mM TRIS).

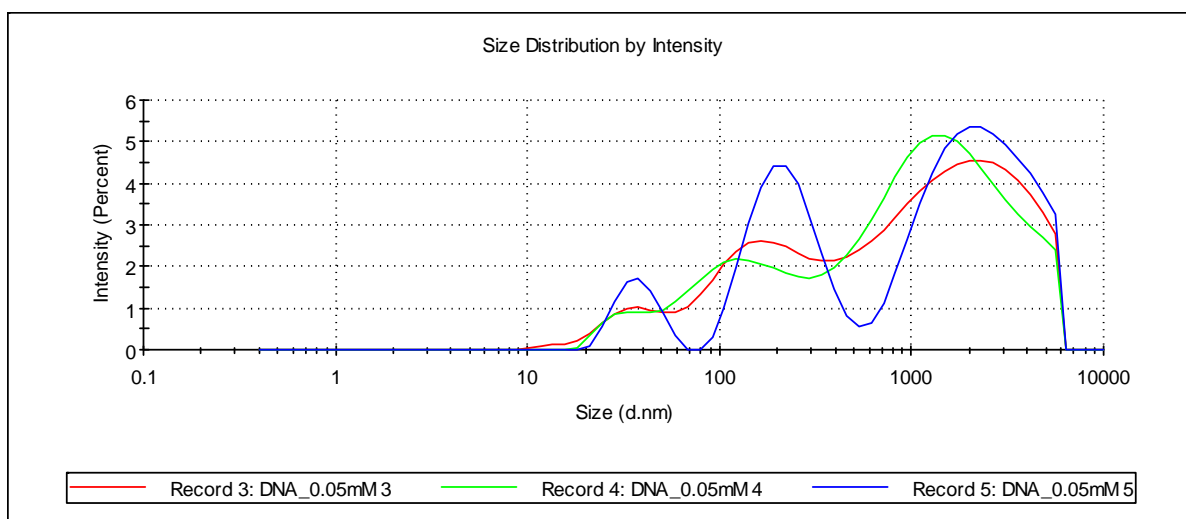


(A)

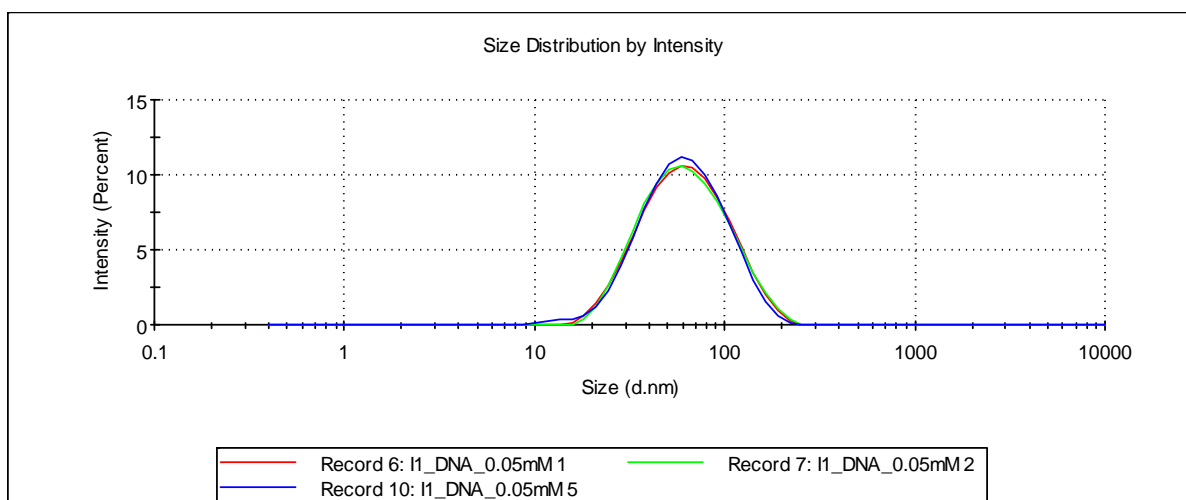


(B)

Figure S7. (A) Stern-Volmer plot of CT-DNA titrated with macrocycles **5-7**. (B) The plot of $-\log[(F_0-F)/F]$ vs $-\log[\text{macrocycle}]$. a – **5**, b – **6**, c – **7**.



(A)



(B)

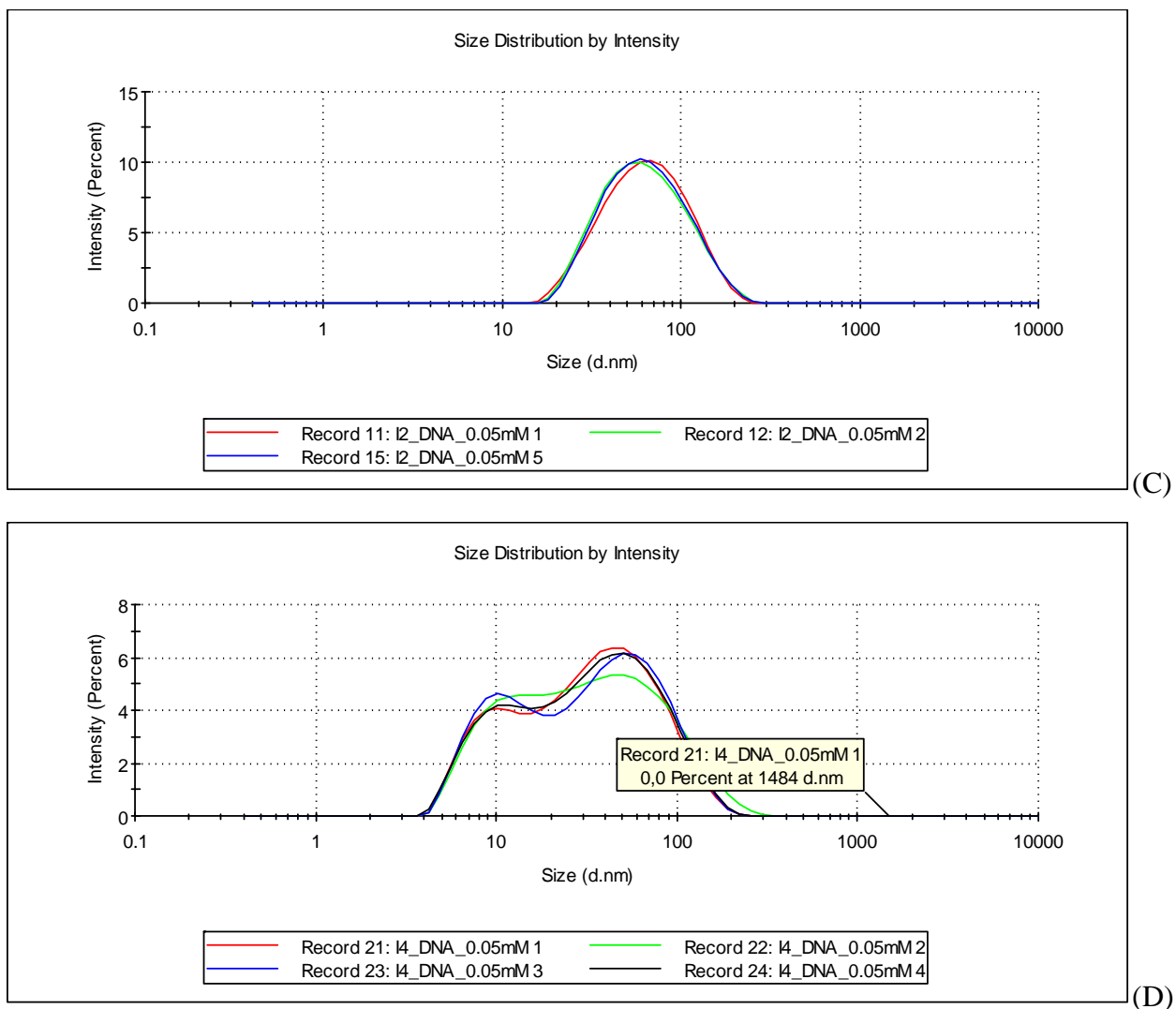


Figure S8. DLS intensity vs diameter graph for solutions of CT DNA (A) and CT-DA with **5** (B), **6**(C) or **7**(D) (C [CT DNA]= 0.05 mM, C [**5-7**] = 0.1 mM, 10 mM TRIS).